ISSN: 0975-8585

Research Journal of Pharmaceutical, Biological and Chemical Sciences

# Study of Gamma Ray Attenuation of High-Density Bismuth Silicate Glass for Shielding Applications.

**Aly Saeed[a], YH Elbashar[b*], and SU El Kameesy[c].**

[a]Basic Science Department, Faculty of Engineering, Egyptian-Russian University-Cairo, Egypt.
[b]Department of Physics, Faculty of Science, Aswan University, Aswan, Egypt.
[c]Department of Physics, Faculty of Science, Ain Shams University, Cairo, Egypt.

**ABSTRACT**

High density glass samples with a chemical formula of $xBi_2O_3$-$30SiO_2$–$10B_2O_3$–20BaO-(40−x)ZnO (where x= 0, 10, 20, 30, and 40 mol %) were prepared using the melt-quenching technique in order to design a new transparently shielding materials for many fields of applications. The amorphous state of the samples was examined using X-ray diffraction technique at room temperature. The effect of bismuth on the structural properties of the studied glasses was characterized through density and its derivative parameters. Before measuring the attenuation capability, the optical transparently for visible light were tested using the transmittance spectra measurements in the UV-Visible region. Optical parameters such as optical band gap, Urbach energy, and refractive index were evaluated from the optical data. The Gamma ray attenuation coefficients of the glass samples were performed at gamma ray energies 238.63, 338.28, 583.19, 911.20, 968.97, 1173.23, 1332.49, and 2614.51 keV that emitted from $^{232}$Th and $^{60}$Co radioactive sources. The transmitted gamma rays were detected using Hyper Pure Germanium detector (HPGe) under good geometry conditions. The Linear attenuation coefficients were deduced from the attenuation curves and then the mass attenuation coefficients and the half value layer were estimated. Theoretical mass attenuation coefficients were calculated using WinXCom program (version 3.1). A good correlation was observed between the experimentally determined and those computed theoretically of the mass attenuation coefficients.

**Keywords:** Radiation shielding materials, optical transmittance, lead free glass.

***Corresponding author***

ISSN: 0975-8585

## INTRODUCTION

Nowadays, the increasing of glass researches due to their applications in photonics and nuclear. The idea of protective materials from nuclear radiation finds increasing interest due to the expansion of using the nuclear technology [1-7]. Glassy materials with the feature of transparency become the most notably materials in respect to their properties which modify their chemical composition by adding some modifiers or intersection to the glass network former [8, 9]. Additionally, the effects of irradiation on the optical, mechanical, and structural properties show an effect to the glass materials [10-12]. The properties of the glassy materials were extensively used as protective materials for multi-nuclear applications [13, 14]. The glass with a heavy metal oxide have several features such as, excellent transparency to visible light (exhibit high refractive index), high viscosity, low glass transition temperature, and high absorption cross-section for nuclear radiation [15-18]. Hence, the purpose of the present work is focused on developing lead free glass containing bismuth due to its high atomic number and hence, strong absorption of gamma rays. Additionally, the toxicity of bismuth and its biological effects were much less than lead [19].

## EXPERIMENTAL

Pure raw materials of $SiO_2$, $H_3BO_3$, $BaCO_3$, ZnO and $Bi_2O_3$ were used in powder form to prepare the glassy samples of chemical composition $xBi_2O_3$-$30SiO_2$–$10B_2O_3$–20BaO-(40 − x) ZnO (where x= 0, 10, 20, 30, and 40 mol %). The glass batches were grind and mixed using a mortar for 30 min to ensure the homogeneity. The melting process of samples was performed in an electric furnace at 1150 $^0$C for 4hrs. The molten was stirred after 3 hrs each 10 min in order to achieve homogeneity. The molten was poured into stainless steel mould and the samples were immediately transferred to a muffle furnace regulated at 360 $^O$C for annealing. After 4 hrs of annealing, the glass samples were allowed to cool after furnace switched off. Finally, samples of cubic shape with dimensions 3x3 cm and different thicknesses were polished using a polishing machine. The amorphous nature of the samples was examined by X-ray diffraction analysis at room temperature using CuKa radiation at λ=1.54 A$^o$ (scintag, advanced diffraction system) with nickel filter, over 2θ range of 3-7 degree. At room temperature the density of the samples was determined by Archimedes principle [20]. The physical properties such as, molar volume, bismuth ion concentration, interionic distance, polaron radius, field strength, and oxygen packing density were evaluated based on the obtained results of density using the standard formulae [20-24].

Optical absorption spectra of these glass samples were recorded using UV-Visible spectrophotometer in the wavelength region 190-1100 nm at nominal incidence. The optical parameters such as, optical band gap, Urbach energy, and refractive index were deduced from the optical absorption data. The gamma ray shielding parameters of the prepared glassy barriers were obtained for eight energy lines, emitted from $^{232}$Th and $^{60}$Co point sources, using narrow beam of gamma rays. The diagram of the geometry was shown in Figure (1). The experimental arrangement consists of Hyper Pure Germanium detector (HPGe) with relative efficiency ≈30% relative to a 3"× 3" NaI (Ti) detector, active volume 62.3 cm$^3$ and energy resolution 1.8 keV at 1.33 MeV γ-lines. The detector was coupled through an amplifier to the computer with MCA plug-in card. Because of the sensitivity of HPGe detector, it is usual to shield them from the environment. Therefore, lead shield of thickness 5 cm was used in this study.

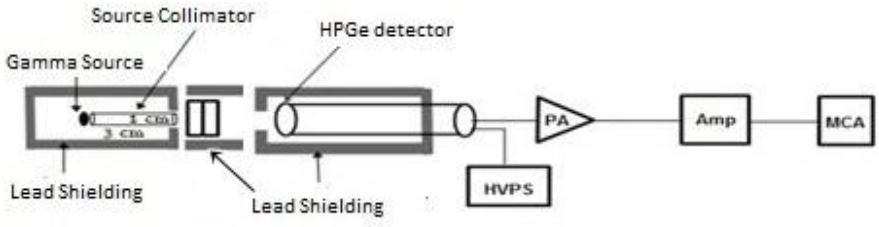


**Figure 1: Experimental setup of narrow beam transmission method.**

## RESULTS AND DISCUSSION

No diffraction peaks were observed in X-ray diffraction patterns of the prepared samples Figure (2) which indicates the amorphous nature of the prepared materials.

ISSN: 0975-8585

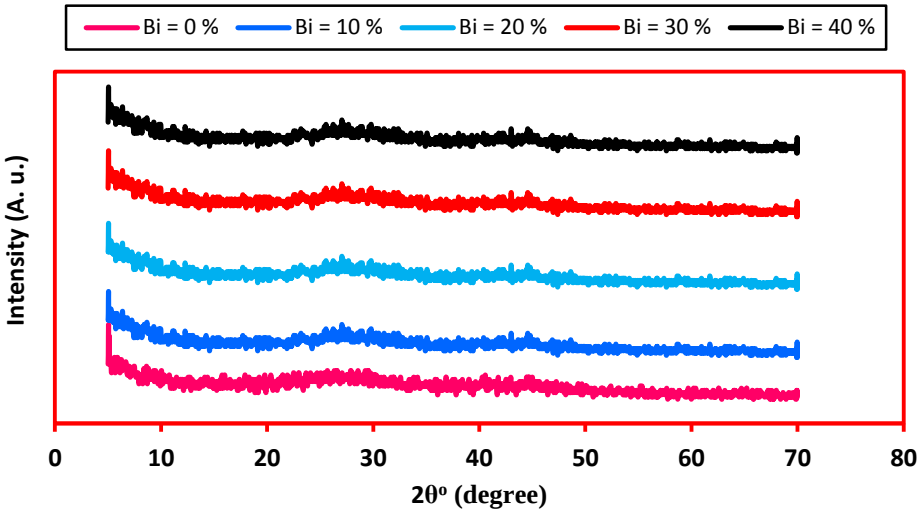


**Figure 2: X-ray diffraction patterns of the studied samples**

Figure (3) shows the behavior of density and molar volume versus bismuth ion concentration. The substituted of ZnO by $Bi_2O_3$ leads to increase the density of glasses due to the high molecular weight of $Bi_2O_3$ in a comparison to ZnO. In the same context, the increasing of molar volume was attributed to creation of non-bridging oxygen in the glass network. The formation of non-bridging oxygen may flayer-up the glass network and this increases its molar volume.

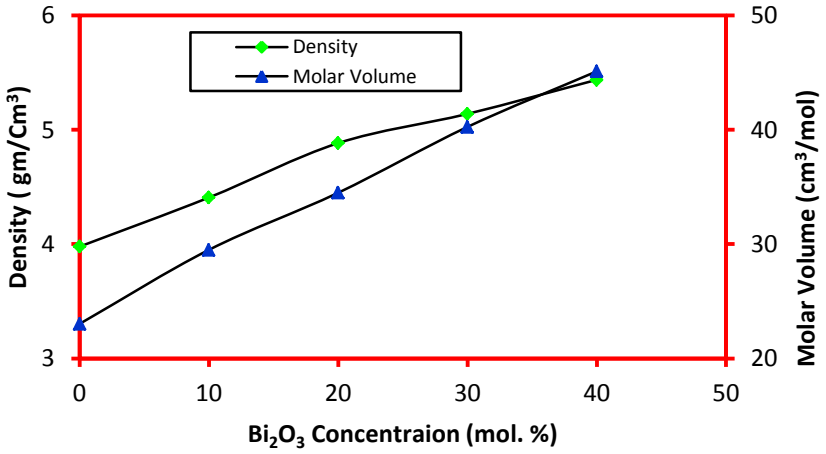


**Figure 3: Density and molar volume of the studied samples**

The better insight, density and molar volume results have been employed to calculate many structural parameters, such as bismuth ion concentration, interionic distance, polaron radius, field strength, oxygen packing density, and number of boned per unit volume, to describe the influence of bismuth ion on the structural units and transport properties of the glasses Table (1).

**Table 1: Optical and structural parameters of the studied glasses**

| | Bi=0% | Bi=10% | Bi=20% | Bi=30% | Bi=40% |
|---|---|---|---|---|---|
| $N_{Bi}$ ×$10^{23}$(ions/$cm^3$) | 0 | 2.041 | 3.492 | 4.489 | 5.341 |
| $r_i$ (Å) | 0 | 1.698 | 1.420 | 1.306 | 1.233 |
| $r_p$ (Å) | 0 | 0.6084 | 0.5072 | 0.5026 | 0.4097 |
| OPD(g-atom/liter) | 65 | 57 | 55 | 52 | 50 |
| $V_O$ ($cm^3$/mol) | 15.355 | 17.355 | 18.154 | 19.168 | 19.614 |
| F×$10^{16}$ ($cm^{-2}$) | 0 | 2.080 | 2.975 | 3.518 | 3.950 |
| $n_b$ ($cm^{-3}$) | 8.891 | 7.348 | 6.635 | 5.985 | 5.608 |
| Eg (eV) | 3.83 | 3.58 | 3.49 | 3.44 | 3.3 |
| $\Delta E$ (eV) | 0.286 | 0.294 | 0.303 | 0.339 | 0.383 |

ISSN: 0975-8585

The polaron radius ($r_p$) and interionic distance ($r_i$) decrease with the increase of bismuth oxide concentration which confirms the increases in bismuth ion concentration ($N_{Bi}$). This behavior indicates that the Bi atoms close to each other which confirm the observed increasing in density. The oxygen molar volume ($V_o$) and oxygen packing density (OPD) values show opposite trend to each other which confirm that the glass structure becomes loosely packed. The increase of field strength attributed to the high field strength of $Bi^{3+}$ in a compare with ZnO. The decrease in the number of bonds per unit volume is attributed to the decrease in the compactness of the glass network structure confirming the formation of non-bridging oxygen.

The transmitted spectra of the investigated glasses were shown in Figure (4). An irregular pattern of optical transmitted spectra was observed with increases of the bismuth concentration. The transmission spectra of the studied glass show that the position of fundamental absorption edge shifts to longer wavelength with $Bi_2O_3$. The variation in optical transmittance spectra and the red shift attributed to the formation of non-bridging oxygen in the glass network.

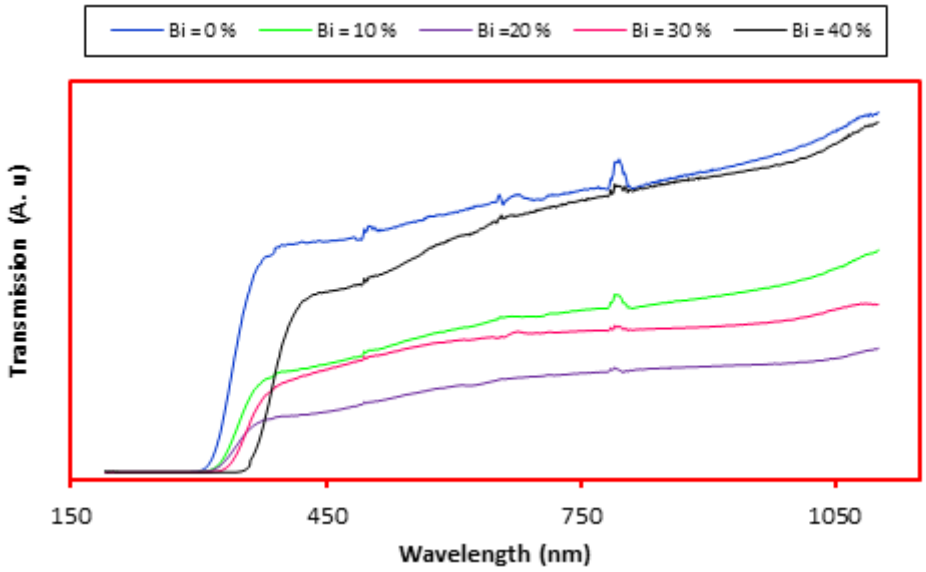


**Figure 4: Optical transmission spectra of the studied samples**

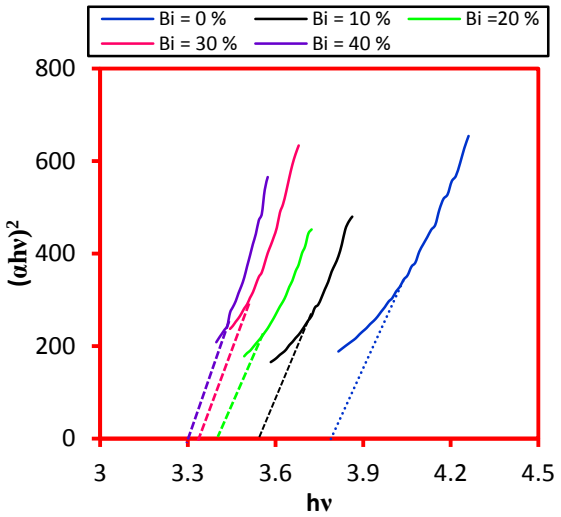


**Figure 5: optical band gap**

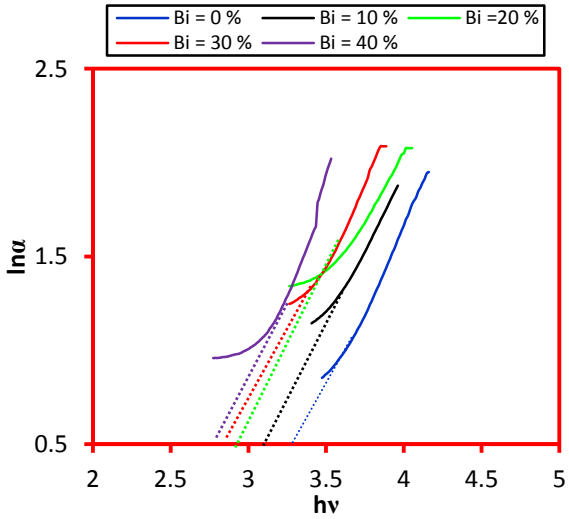


**Figure 6: Urbach enrgy**

The optical band gap energy for direct transition is determined using the plot $(\alpha h\nu)^2$ versus energy $(h\nu)$ as shown in Figure (5). From the linear extrapolation to zero ordinate the values of $E_g$ was calculated [17-

19]. Urbach energy (ΔE) obtained from the slope reciprocal of the graph of absorption coefficient logarithm ($\ln \alpha$) versus the photon energy ($h\nu$) [17-19] as shown in Figure (6). The obtained results of optical band gap and Urbach energy are listed in Table (1). It is found that the optical band gap energy decreases and the Urbach energy increases with the increase of bismuth ion concentration. The observed behavior of direct optical band gap can be attributed to the increase in non-bridging oxygen with the increase in bismuth content. The decrease in $E_{opt}$ values and increase in Urbach energies confirm the increase of disorder in the glass network, and consequently the extension of the localized states within the band gap.

Refractive index based on the optical band gap was estimated, to confirm the transparently of the prepared glasses, with according following relation [17-21].

$$\frac{n^2-1}{n^2+1} = 1 - \sqrt{E_g/20} \qquad (1)$$

The refractive index values for the studied glasses, as shown in Figure (7), increase with bismuth oxide increase. This behavior is due to the ion $Bi^{3+}$ which has a high polarity that can break the bridging oxygen in glass network to non-bridging oxygen [NBO]. Non-bridging oxygen has an effect on the refractive index because of the high polarity of non-bridging oxygen (NBO) than the bridging oxygen.

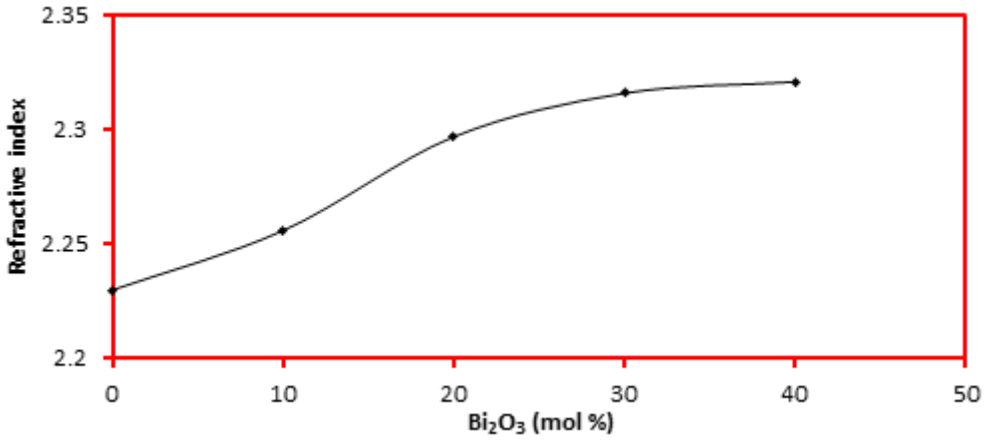


**Figure 7: Refractive index of the present glasses**

The values of linear attenuation coefficients (μ) were plotted versus bismuth concentration (Bi %) and the energy lines of γ-rays as shown in Figures (8 and 9). The linear attenuation coefficient of all glass barriers increase linearly with increasing Bi concentration, and it is also observed that the linear attenuation coefficient are inversely proportional to energy. The observed behavior of linear attenuation coefficients attributed to the higher molecular weight of bismuth as well as, the mechanism of gamma ray interaction with the materials.

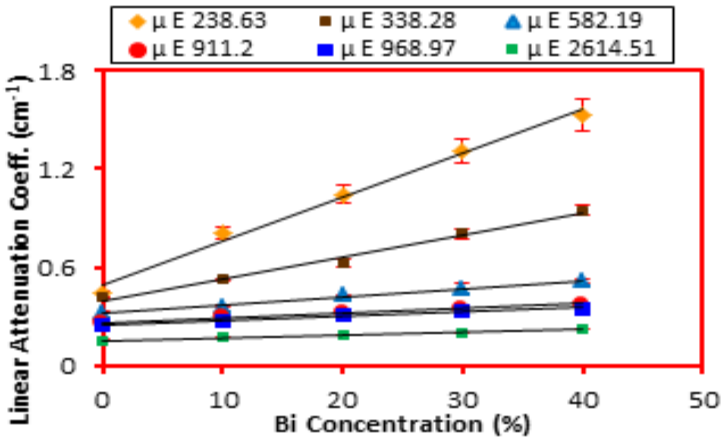


**Figure 8: Linear attenuation coefficients of γ-rays emitted from $^{232}$Th source**

ISSN: 0975-8585

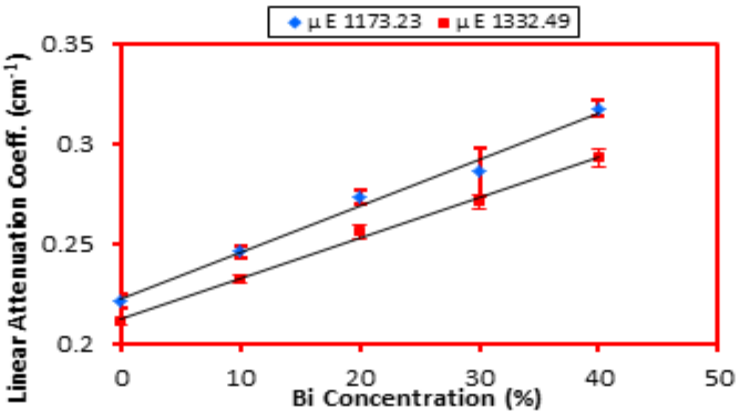


**Figure 9: Linear attenuation coefficients of γ-raysemitted from $^{60}$Co source**

.

The experimental and theoretical results of mass attenuation coefficients ($\mu_{exp}$ $and$ $\mu_{th}$) as a function of gamma ray energies, were investigated for the glassy barriers as shown in Figure (10). Two different regions were observed in the behavior of mass attenuation coefficients. The energy range from 238.63 keV up to 583.19 keV a sharp decrease of mass attenuation coefficients was observed because of the dominant reaction between the investigated glass barriers and gamma rays was attributed to the photoelectric effect. A slight decrease of mass attenuation coefficients is observed from 911.2 keV up to 2614.51 keV which was attributed to the Compton scattering process. Additionally, Figure (10) show a good agreement between the experimental and the theoretical predictions.

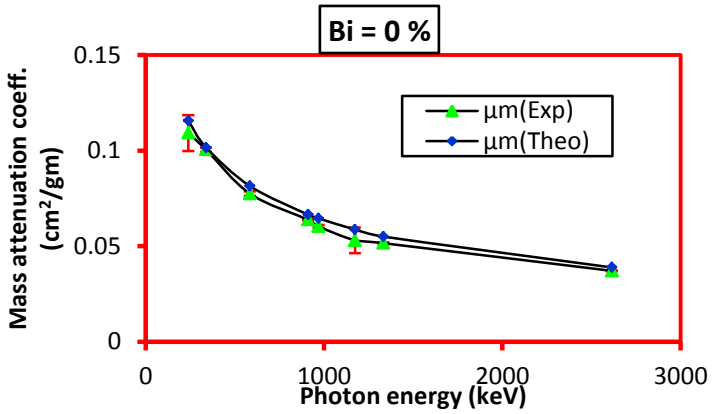


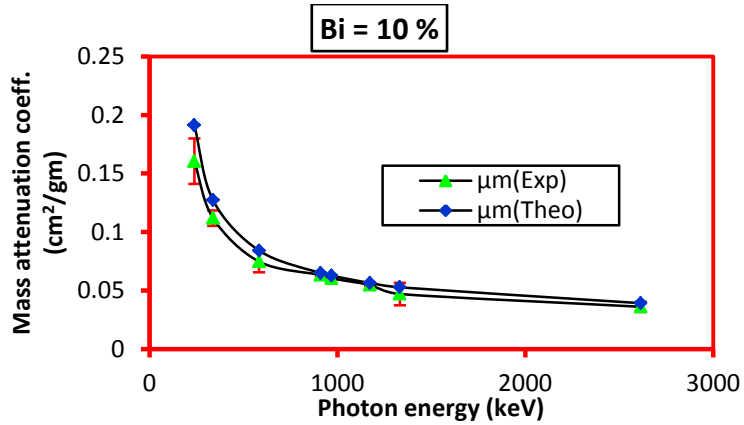

ISSN: 0975-8585

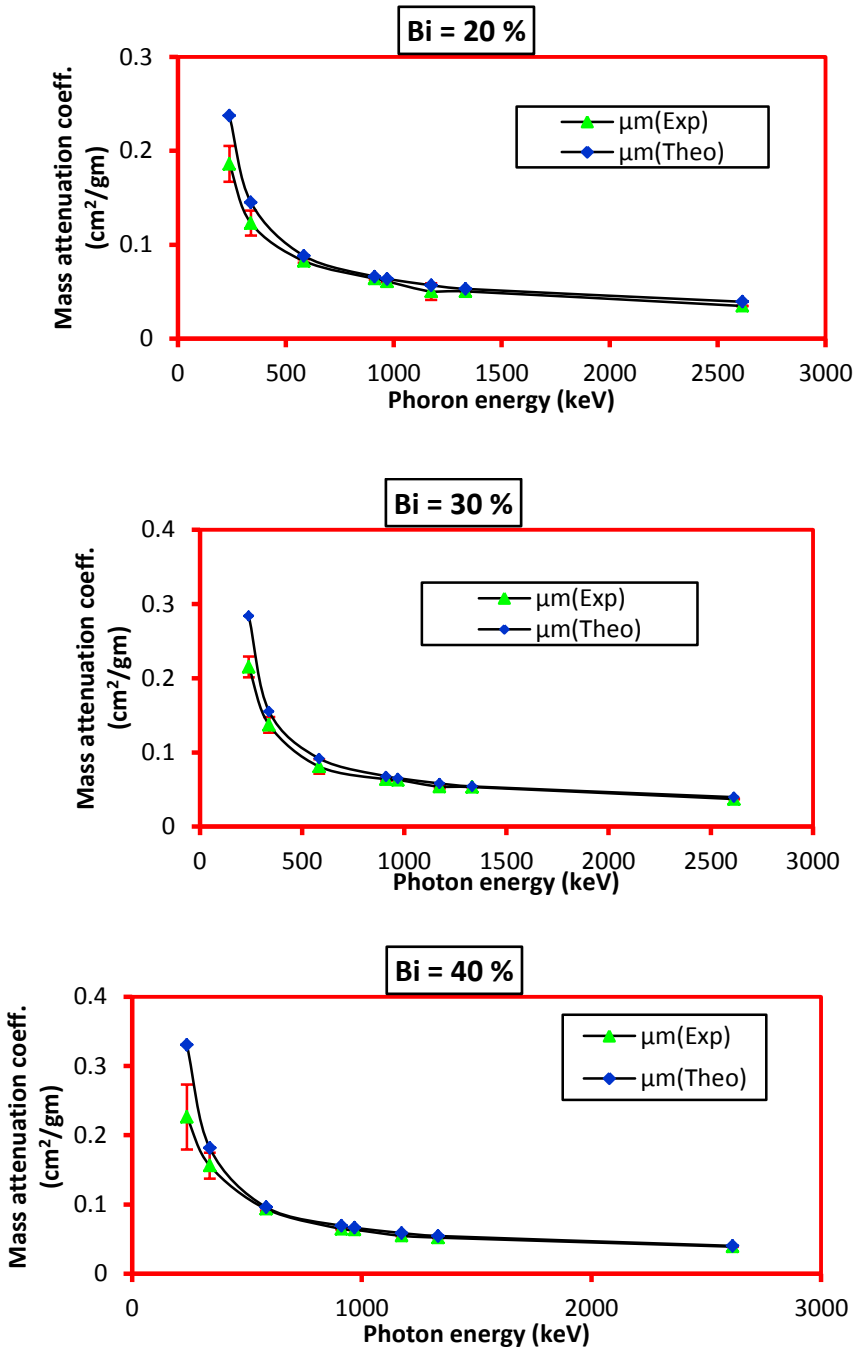


**Figure 10: Mass attenuation coefficients of glassy samples as a function of gamma ray energies.**

**Table 2: Half value layer (HVL) for the investigated glass barriers**

| γ- Energy (keV) | 0 % (Bi) | 10 % (Bi) | HVL 20 % (Bi) | 30 % (Bi) | 40 % (Bi) | $\left(\frac{HVL_{0\%} - HVL_{40\%}}{HVL_{0\%}}\right) * 100$ |
|---|---|---|---|---|---|---|
| 238.63 | 1.583 | 0.837 | 0.656 | 0.523 | 0.441 | 72.226 |
| 338.28 | 1.654 | 1.328 | 1.142 | 0.866 | 0.733 | 55.661 |
| 583.19 | 2.166 | 1.964 | 1.716 | 1.530 | 1.389 | 35.871 |
| 911.20 | 2.718 | 2.295 | 2.094 | 2.009 | 1.810 | 33.420 |
| 968.97 | 2.888 | 2.358 | 2.194 | 1.942 | 1.889 | 34.604 |
| 1173.23 | 3.136 | 2.876 | 2.530 | 2.318 | 2.181 | 30.503 |
| 1332.49 | 3.180 | 2.795 | 2.636 | 2.424 | 2.334 | 26.599 |
| 2614.51 | 4.814 | 4.151 | 3.747 | 3.591 | 3.194 | 33.640 |

The values of the half value layer for the present glassy barriers were deduced and listed in Table (2). The decrease of half value layers, with the bismuth concentration increase, indicates the improvement of shielding properties for the present glasses.

## CONCLUSION

Attenuation coefficients of $xBi_2O_3$–$30SiO_2$–$10B_2O_3$–20BaO–(40–x) ZnO glass system have been measured using collimated gamma ray transmission method. The results show a clear improvement in shielding parameters by increasing $Bi_2O_3$ concentration up to 40%. The optical transmission spectra have been studied and analyzed. The band gap value decreases and the refractive index increase with the incorporation of $Bi_2O_3$. It may be attributed to the compaction of glass structure and formation of non-bridging oxygen. The influence of $Bi_2O_3$ on the glass structure was studied using density, molar volume, bismuth ion concentration, and oxygen packing density. The structural properties of these glasses confirm the creation of non-bridging oxygen in the glass network. Moreover, the present study shows that the bismuth borosilicate glass for gamma ray shielding material is suitable, and promising transparently radiation protecting materials which have a wide range of applications.

## REFERENCES


[1] Eskandar Asadi Amirabadi, Marzieh Salimi, Nima Ghal-Eh, Gholam Reza Etaati, and Hossien Asadi. Int J Inn App Stud 2013;3(4):1079-1085.
[2] Aly Saeed, et al. Rad Phy Chem 2014;102:167-170.
[3] DA Rayan, YH Elbashar, AB El Basaty and MM Rashad. Res J Pharm Biol Chem Sci 2015;6(3):1026-1030.
[4] H Elhaes, M Attallah, Y Elbashar, M Ibrahim, M El-Okr. J Physica B: Cond Matter 2014;449:251–254.
[5] Nehal Aboulfotoh, Yahia Elbashar, Mohamed Ibrahem, Mohamed Elokr. Journal of Ceramics International ,Volume 40, Issue 7, Part B, August 2014, Pages 10395–10399
[6] Hanan Elhaes, Mohamed Attallah, Yahia Elbashar, Ayser Al-Alousi, Mohamed El-Okr, and Medhat Ibrahim. J Comp Theoretical Nanosc 11 (10):2079-2084
[7] DA Rayan, YH Elbashar, MM Rashad, and A El-Korashy. J Non-crystalline Solids 2013;382:52–56.
[8] S Kaewjaeng, J Kaewkhaob, P Limsuwan, and U Maghanemi. Procedia Eng 2012;33:1080-1086.
[9] Aleksander Samarin. Energy and Environmental Engineering 2013;1(2):90-97.
[10] MS Hossain, SM Islam, MA Quasem, and MA Zaman. Indian J Pure App Phy 2010;48:860-868.
[11] Marzieh Salimi, Eskandar Asadi Amirabad, Nima Ghal-Eh, Zahra Soltani, and Gholamreza Etaati. Int J Inn App Stud 2013;4(2):437-440.
[12] Sandeep Gupta and Gurdeep Singh Sidhu. International Journal of Scientific and Research Publications 2012;2:1-7.
[13] J Kaewkhao, A Pokaipisit, and P Limsuwan. Journal of Nuclear Materials Vol. 399, 38–40, 2010.
[14] Suparat Tuscharoen, Jakrapong Kaewkhao, Pichet Limsuwan, and Weerapong Chewpraditkul. Prog Nuclear Sci Technol 2011;1:110-113.
[15] Nattha kridtachanthima, Jakrapong Kaewkhao, Chittra Kedkaew, Weerapong Chewpraditkul, Artorn, Pokaipisit, and Pichet Limsuwan. Prog Nuclear Sci Technol 2011;1:106-109.
[16] Sandeep Kaur and KJ Singh. Ann Nuclear Energy 2014;63:350–354.
[17] P Limkitjaroenporn, J Kaewkhao, P Limsuwan, and W Chewpraditk. J Phy Chem Solids 2011;72:245–251.
[18] Samir Yousha El-Kameesy, SaharAbd El-Ghany, Moenis Abd El-Hakam Azooz, and Yaser Abd Allah El-Gammam. World Journal of Condensed Matter Physics 2013;3:198-202.
[19] Sandeep Kaur, KJ Singh, Rajinder Singh Kaundal, Vikas Anand, and Kulwinder Kaur. Asian J App Sci 2013;1:99-103.
[20] Smit Insiripong, Parnuwat Chimalawong, Jakrapong Kaewkhao, and Pichet Limsuwan. American J App Sci 2011;8(6):574-578.
[21] DP Singh and Gurinder Pal Singh. J Alloys Comp 2013;546:224–228.
[22] M Prajna Shree, et al. European Sci J 2013;9(18): 83-92.
[23] M Çelikbilek, AE Ersundu, and S Aydin. J Non-Crystalline Solids 2013;378:247–253.
[24] Asha Rajiv, M Sudhakara Reddy, Jayagopal Uchil, C Narayana Reddy. J Adv Sci Res 2014;5(2):32-39.